Effectiveness of various dispersed alkaline substrates for the pre-treatment of ferriferous acid mine drainage

Tsiverihasina V. Rakotonimaro [a], Carmen Mihaela Neculita [a, *], Bruno Bussière [a], Gérald J. Zagury [b]

[a] Research Institute on Mines and Environment (RIME)-University of Quebec in Abitibi-Temiscamingue (UQAT), Rouyn-Noranda, QC, Canada
[b] RIME- Polytechnique Montreal, Department of Civil, Geological, and Mining Engineering, Polytechnique Montreal, Montreal, QC, Canada

A R T I C L E   I N F O

A B S T R A C T

Dispersed alkaline substrates (DAS) have been successfully used in passive treatment of highly contaminated acid mine drainage (AMD) to limit coating and clogging issues. However, further optimization of DAS systems is still needed, especially for their long-term efficiency during the treatment of ferriferous AMD. In the present study, three types of DAS comprised of natural alkaline materials (wood ash, calcite, dolomite), in different proportions (20%v/v, 50%v/v, 80%v/v), and a substrate with high surface area (wood chips) were tested in 9 batch reactors. The testing was carried out, in duplicate, for a period of 91 days, to evaluate the comparative performance of the mixtures for iron pre-treatment in ferriferous AMD (2500 mg/L Fe, at pH 4). Results showed increasing of pH (between 4.15 and 7.12), regardless of the proportion of alkaline materials in the DAS mixtures. Among the tested mixtures, wood ash type DAS were more effective for Fe removal (99.9%) than calcite or dolomite type DAS (up to 66%). All tested DAS had limited efficiency for sulfate removal and an additional treatment unit, such as a sulfate-reducing biochemical reactor, is needed. Moreover, due to the similar performances of the calcite and dolomite DAS, they could be potentially substituted and rather be used in a polishing treatment unit. Based on these findings, the most promising mixture was the 50% wood ash type DAS (WA50-DAS).

© 2016 Elsevier Ltd. All rights reserved.

1. Introduction

Environmental impacts of acid mine drainage (AMD), which is characterized by low pH ($-3.6 < pH < 6$) and high concentrations of dissolved metals, metalloids and sulfate (SO_4^{2-}) are largely documented (Neuman et al., 2014; Nordstrom et al., 2015). Improvement of technologies has been conducted over the last decade to limit and prevent AMD generation (Sahoo et al., 2013; Jennings and Jacobs, 2014). Several treatment technologies, including active and passive systems, have also been developed (USEPA, 2014). Passive treatment is preferred, principally for moderately contaminated water, because of its low cost, potential production of marketable sludge, and simple installation and operation (Hedin et al., 2013; Zipper and Skousen, 2014). Despite these advantages, efficiency of a single unit of passive treatment (e.g. oxic/anoxic limestone drains- OLD/ALD, passive biochemical reactor- PBR) is limited when used for the treatment of highly contaminated AMD, particularly ferriferous AMD (Fe > 500 mg/L) (Neculita et al., 2008; Genty et al., 2010). Hence, combinations of two or more units of passive treatment or so-called passive multi-step treatment system have been developed (Macías et al., 2012; Genty et al., 2012a). Nonetheless, coating/passivation (loss of reactivity) and clogging (loss of permeability) caused by precipitated minerals during treatment (e.g. gypsum, metal oxide-hydroxides) (Rötting et al., 2008a) are presently limiting the long term performance of such systems. Their longstanding efficiency is conditioned by removal, at an early stage, of acidogenic metallic elements, such as Fe and/or Al (Ayora et al., 2013). Indeed, during precipitation of ferric iron as hydroxide [$Fe(OH)_3$] (Eq. (1)), which starts at pH around 3—3.5, depending on Fe total concentration, the pH decreases, and the removal of divalent metals (which precipitation requires pH > 8.5), is inhibited.

$$Fe^{3+} + 3H_2O \rightarrow Fe(OH)_3 + 3H^+ \tag{1}$$

Consequently, a pre-treatment unit for Fe removal in ferriferous AMD is a must before forwarding water into a second treatment unit for the removal of other metals and of SO_4^{2-}, if necessary. Various techniques have been developed for Fe pre-treatment, such as oxidation/precipitation (Champagne et al., 2008), oxic limestone drain (OLD) (Figueroa et al., 2007), natural Fe-oxidizing lagoon (NFOL) (Macías et al., 2012), and cascade aeration (USEPA, 2014). Most of these techniques gave promising results, but have been mostly used for Fe pre-treatment when AMD has low to moderate concentrations (40−1000 mg/L Fe). Regarding Fe concentration, the quality of water in this study is then considered as extremely contaminated (2500 mg/L Fe).

Innovative approaches using reactive mixtures composed of a coarse, highly porous material (wood chips) and small grain size of neutralizing agents (e.g. MgO, $CaCO_3$) known as dispersed alkaline substrate (DAS) have also been investigated with the aim of overcoming the coating-clogging general issues in passive treatment (Macías et al., 2012; Ayora et al., 2013). Two main types of DAS have been used to treat AMD, one comprised of MgO (MgO-DAS), for the removal of bivalent metals (e.g. Macìas et al., 2012; Ayora et al., 2013), and one of calcite (calcite-DAS), for the removal of trivalent metals (e.g. Rötting et al., 2008b; Caraballo et al., 2011).

In passive treatment, the use of economic, available and natural materials or substitute is recommended. Other selection criteria include the reaction rate of neutralizing agents, sludge production and costs (Potgieter-Vermaak et al., 2006). Hence, the dolomite DAS could be an economic replacement of the calcite/limestone DAS because it could reduce expenses up to 23% (Potgieter-Vermaak et al., 2006). Moreover, previous studies using dolomite as a neutralizing agent in the treatment of very acidic water have shown promising results (Potgieter-Vermaak et al., 2006; Huminicki and Rimstidt, 2008; Genty et al., 2012a). Depending on the grain size, some studies even presented comparable efficiency of calcite and dolomite when used for the treatment of moderately contaminated AMD under anoxic condition, with lower difference in alkalinity production (105−220 mg/L as $CaCO_3$) for a hydraulic retention time of 15 h (Genty et al., 2012a). Additional benefits of dolomite-DAS include the delaying of the neoformed minerals (e.g. gypsum $CaSO_4 \cdot H_2O$) because of the belated release of Ca^{2+}.

Another potential replacement of MgO in DAS systems could be wood ash, principally used for its high pH (up to 12), metal retention, and neutralization capacity. The wood ash, which is usually considered as a waste, has in fact a good potential of reuse. It showed efficiency in the pre-treatment of ferriferous AMD (Genty et al., 2012b). Moreover, it is an economic material, relative to MgO which cost is up to ten times higher than limestone (Rötting et al., 2006). Then, wood ash-DAS (WA-DAS) could be advantageous and potentially give similar performance to MgO-DAS. Despite the satisfactory performance (in terms of Fe and SO_4^{2-} removal, as well as of hydraulic conductivity stability) of the wood ash, its long term performance remains uncertain (Genty et al., 2012b). Moreover, additional treatment units for sulfate removal are necessary.

The results of a very recent laboratory study, which compared the performance of calcite-DAS to witherite ($BaCO_3$)-DAS, in terms of SO_4^{2-} removal, showed that the last was more efficient, but became unreactive after only 40 days of operation, due to passivation (by coating with barite − $BaSO_4$) (Lozano et al., 2015).

Therefore, the objective of the present study is to evaluate the efficiency of WA-DAS, calcite-DAS and dolomite-DAS in batch testing, in the perspective of their use as pre-treatment units for Fe removal in a ferriferous AMD. The residual Fe concentration targeted for this pre-treatment is 500 mg/L. This concentration was reported as a threshold value based on the steady performance of a PBR, in a 15-month laboratory study (Neculita et al., 2008).

2. Materials and methods

2.1. Physicochemical characterization of materials composing the mixtures

Nine reactive mixtures made of natural materials, i.e. wood chips, and three neutralizing agents (wood ash, calcite and dolomite) were evaluated in batch tests. The wood ash was a by-product from a co-generation plant located at Kirkland Lake (Canada), the wood chips originated from P.W.I. industries (QC), the calcite from the quarry of Perth (ON), and the dolomite from the Temiscamingue region (QC). These three reagents were mainly composed of Ca and Mg (Table 1, Supplementary material). Grain size of calcite and dolomite was less than 5 mm, in order to allow almost complete dissolution, before eventual armoring during the treatment of ferriferous AMD. In this study, paste pH of the nine mixtures was determined in deionized water using a solid liquid ratio of 1:10 (ASTM, 1995). Water content was evaluated in duplicate by drying samples at 40 °C during 2 days. Specific surface area (Ss) of dry samples was determined by the BET method using 5-point N_2 adsorption isotherms with Micromeritics Gimini III 2375 surface analyzer. Particle size analysis was carried out using standard sieves (ISO R-20) in order to obtain size corresponding to 10% and 60% by weight of passing, as well as uniformity coefficient (D_{10}, D_{60} and $C_u = D_{60}/D_{10}$ respectively) (Aitcin et al., 2012). Loss on ignition (LOI), used as an indication of the organic matter content, was determined by weighing the samples before and after calcination (375 °C for 16 h). Each mixture was grinded and sieved through 0.25 mm opening before being digested in a mixture of strong mineral acids (HNO_3, Br_2, HCl, and HF) (Potts, 1987). Then, the resulting digestate was analyzed for Fe, Ca, Mg and SO_4^{2-} content by Inductively Coupled Plasma-Atomic Emission Spectrometry (ICP-AES; relative precision of 5%) using a Perkin Elmer OPTIMA 3100 RL.

2.2. Batch testing description

The nine mixtures were set up in duplicate in 18 glass flasks of 1 L, at room temperature (around 20 °C). Each batch reactor was filled with 200 g dry mixture and 600 mL synthetic AMD (Neculita and Zagury, 2008). Mixtures consisted of wood chips and one of the following three neutralizing agents: wood ash (WA-DAS), calcite (calcite-DAS) or dolomite (dolomite-DAS) (Table 1). The batch testing was performed during a 91-day period.

The characteristics of synthetic AMD (Table 2) simulated the typical water quality of ferriferous AMD encountered at several closed/abandoned mine sites in the region of Abitibi-

Table 1
Composition and relative proportion of components of the nine reactive mixtures tested in batch reactors.

Reactors	Wood ash	Calcite	Dolomite	Wood chips	Total
	(%v/v)				
WA20	20	–	–	80	100
WA50	50	–	–	50	100
WA80	80	–	–	20	100
C20	–	20	–	80	100
C50	–	50	–	50	100
C80	–	80	–	20	100
D20	–	–	20	80	100
D50	–	–	50	50	100
D80	–	–	80	20	100

WA: Wood ash; C: Calcite; D: Dolomite.

Table 2
Physicochemical quality of synthetic ferriferous AMD used in batch testing.

Parameter	Concentration (mg/L, excepting for pH)	Source
Al	1.6 ± 0.6	$Al_2(SO_4)_3 \cdot 18H_2O$
Fe	2500 ± 300	$FeSO_4 \cdot 7H_2O$
Mg	33.5 ± 3.8	$MgSO_4 \cdot 7H_2O$
Mn	8.2 ± 1.0	$MnSO_4 \cdot H_2O$
Ni	0.7 ± 0.4	$NiSO_4 \cdot 6H_2O$
Pb	0.2 ± 0.1	$Pb(NO_3)_2$
Zn	0.2 ± 3.0	$ZnSO_4 \cdot 7H_2O$
Ca	430 ± 5	$CaSO_4 \cdot 2\,H_2O$
SO_4	5395 ± 1000	$Na_2SO_4 \cdot 10H_2O$
pH	4	—

Temiscamingue (QC, Canada), in Canada and around the world (Genty et al., 2012a; Ayora et al., 2013; Bejan and Bunce, 2015).

2.3. Sampling, analysis and geochemical modeling

Measurements of pH, redox potential (Eh), electrical conductivity (EC) and dissolved oxygen (DO), as well as analysis of alkalinity, acidity, total iron (Fe_t), ferrous iron (Fe^{2+}) and SO_4^{2-} concentrations were performed weekly, over the entire testing period. Water pH was measured with an electrode AccupHast 13-620-114 ATC/BNC, while the EC was measured with an Accumet 13-620-100 electrode. The two electrodes were connected to an Accumet Excel XL-60®. Redox potential was measured with a potentiometer (Sension1 POR HACH 51939-00) coupled with an internal Pt/Ag/AgCl electrode (dipped in acid 1N solution). The reading was then corrected relative to the standard hydrogen electrode (SHE) to calculate the Eh. The DO was measured using a LDO10103-Hack HQ30d probe, calibrated with air-saturated water. Alkalinity and acidity were determined with a Metrohm Binkmann, 716 DMS Trinitro titrator (APHA, 2005). The concentrations of Fe_t, Fe^{2+} and SO_4^{2-} were determined on filtered samples (0.45 μm), within the first 2 h after collection, with a DR/890 HACH colorimeter (Method 8008−1, 10 phenantroline, Method 8146−1, 10 phenantroline, and Method 8051− barium chloride powder pillows for Fe_t, Fe^{2+} and SO_4^{2-}, respectively). Total metal concentrations were analyzed by ICP-AES, at the beginning and at the end of the experiments, on filtered (0.45 μm) and acidified (with 2% (v/v) of nitric acid) samples.

Following these analysis, relative metal removal r (%) in the supernatant was calculated using the following equation:

$$r = [(C_x - C_{x+7})/\, C_x].\,100$$

where C_x and C_{x+7} are metal concentrations (mg/L) at time x and $x+7$ days. Precipitated Fe was calculated from the difference between the Fe_t content of water at t_x and at t_{x+7}.

Metal removal mechanisms during the batch testing were evaluated using the physicochemical quality of supernatant samples collected on days 0, 7, 14, 21, 56, 70 and 91 and the geochemical equilibrium software VMINTEQ, version 3.0 (KTH, 2013).

2.4. Post-testing mineralogy

Samples were collected from the batch reactors and dried at 40 °C for 48 h and metallized. Afterward, the microstructure and mineralogy were observed with a scanning electron microscope (SEM) equipped with probe Energy dispersive X-ray spectroscopy (EDS) HITACHI S-3500N (voltage of 20 kV, amperage of 140 A, pressure around 25 kPa and work distance of 15 mm). Images, element maps and chemical composition were recorded with a data processor INCA (Oxford Energy 450).

Crystalline phases of the secondary precipitates were analyzed by X-ray diffraction (XRD, Bruker axs D8 ADVANCE) equipped with a Cu anticathode and a scintillation counter. Prior to XRD analyses, the samples were dried (at 40 °C for 48 h), and grinded to 10 μm (detection limit <1%w/w). Then, the data was collected and interpreted for minerals identification and quantification with Bruker axs EVA and TOPAS software packages.

3. Results and discussion

3.1. Physicochemical characteristics of the substrates

Initial pH of WA-DAS was higher (7.98−9.41) than both calcite- and dolomite-DAS (6.02−8.80) (Table 3). In addition, water content was higher for WA-DAS (18.3−28.3%) than for calcite- or dolomite-DAS (0.3−2.2%), indicating that the materials composing these two last DAS were dry. Specific surfaces (Ss) of calcite- and dolomite-DAS were relatively low (0.16−0.55 m²/g) comparing to that of WA-DAS (9.15−32.50 m²/g). Nonetheless, the dolomite-DAS had double Ss relative to calcite-DAS, except for the C20 mixture (Table 3). The Ss of calcite-DAS was higher (0.16−0.46 m²/g) compared to calcite alone with similar particle size, as reported in a previous study (12.07×10^{-4} m²/g, Genty et al., 2012a). The wood chips might have contributed to this Ss increase. Calcite- and dolomite-DAS had spread grains size distribution and contained low fines ($D_{10} = 0.18-0.26$ mm, $D_{60} = 0.7-1.4$ mm, Cu = 3.18−6.36). On the contrary, the WA-DAS contained considerable fraction of fines as the proportion of wood ash in the mixture was high ($D_{10} = 4-22$ μm, $D_{60} \approx 0.3-0.4$ mm, Cu = 1.45−150), which explain, at least in part, its high Ss value. Mixtures composed of wood ash also had higher organic contents as indicated by the results on LOI, which were 2−3 times higher for WA20 compared to C20 and D20, 5 times higher for WA50 compared to C50 and D50, and 7 to 13 times higher for W80 compared to C80 and D80
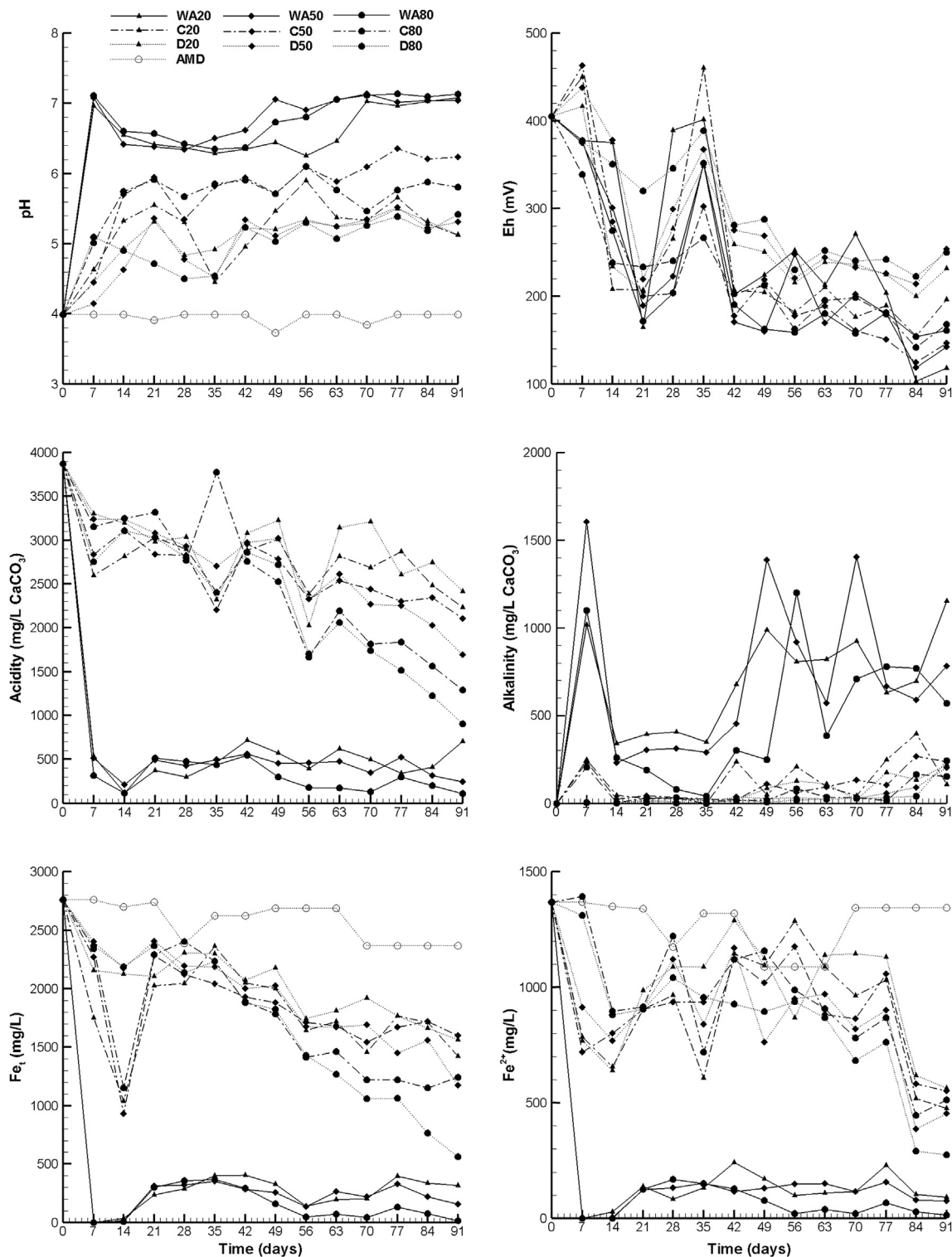
Table 3
Physicochemical characteristics of substrates used in batch testing.

Mixtures	pH	Ss (m²/g)	Water content (%w/w)	LOI (%)	Ca	Mg	Fe	SO_4^{2-}
					(g/kg)			
WA20	7.98	9.15	28.3	78.6	28	2.4	<0.01[a]	0.9
WA50	8.79	18.63	18.3	63.4	50	5.6	<0.01	3.4
WA80	9.41	32.8	22.0	46.8	91	9.5	11.1	7.8
C20	6.51	0.46	1.8	28.3	170	0.5	<0.01	0.9
C50	7.41	0.21	0.8	12.0	224	1.3	<0.01	0.9
C80	8.73	0.16	2.0	6.6	300	5.5	<0.01	0.9
D20	6.02	0.43	2.2	44.3	115	65.0	<0.01	0.9
D50	8.02	0.43	1.0	12.6	354	55.0	<0.01	0.9
D80	8.80	0.55	0.3	3.5	182	53.0	<0.01	0.9

[a] Method detection limit.

Fig. 1. Evolution of pH, Eh, acidity, alkalinity, Fe_t and Fe^{2+} concentration in wood ash-, calcite- and dolomite-DAS batch reactors.

(Table 3). The results on water content and LOI indicate the presence of significant organic carbon in all mixtures, particularly in WA-DAS, originating mainly in the wood chips and probably with the contribution of unburned wood contained in the wood ash itself (Genty et al., 2012b). Thus, sorption of metallic ions on negatively charged surface of organic material components could be a resulting advantage (Asadi et al., 2009). The Ca content of WA-DAS was 2–7 times lower than of calcite- and dolomite-DAS. Mg content of dolomite-DAS was 10–130 times higher than in calcite-DAS and 6 to 27 higher than in the WA-DAS. A higher release of Mg^{2+} from dolomite could induce higher SO_4^{2-} removal (>86% at 300 mg/L Mg^{2+}; Potgieter-Vermaak et al., 2006). This could be partially explained by potential reaction of Mg^{2+} with SO_4^{2-} and/or HCO_3^- to form either $MgSO_4$ or $MgCO_3/Mg(HCO_3)_2$, with respect to pH (Eq.
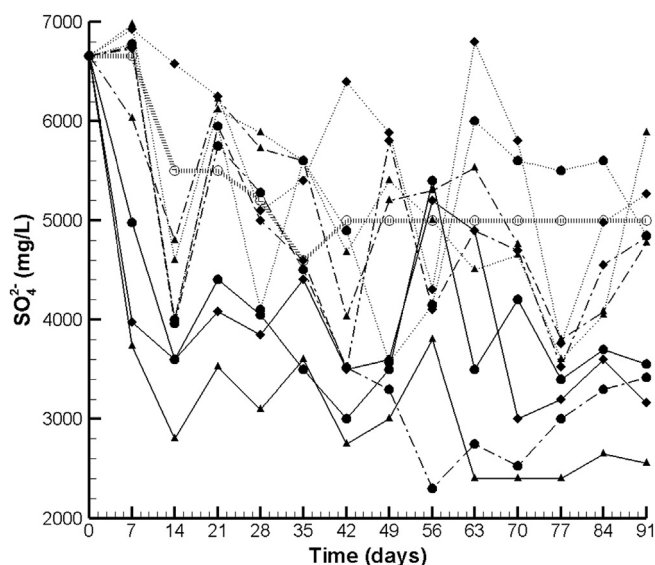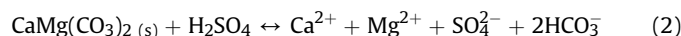
Fig. 2. Evolution of SO_4^{2-} concentration in wood ash-, calcite- and dolomite-DAS batch reactors.

(2)). Since $MgSO_4$ is soluble in water, the formation of insoluble $MgCO_3/Mg(HCO_3)_2$ would be favored. Consequently, Ca^{2+} would be available to form $CaSO_4$ or gypsum.

$$CaMg(CO_3)_{2\,(s)} + H_2SO_4 \leftrightarrow Ca^{2+} + Mg^{2+} + SO_4^{2-} + 2HCO_3^- \qquad (2)$$

These results might give calcite- and dolomite-DAS the advantage to delay Fe-oxide-hydroxides precipitation that entails clogging issues in comparison to WA-DAS. All substrates contain low Fe and have similar concentrations of SO_4^{2-}, except for WA50 and WA80 (Table 3). Noteworthy, significant SO_4^{2-} concentrations were released in control batch (set up with deionized water slightly acidified with sulfuric acid to maintain a pH around 4, for 24 h and 1 week) with respectively 220 mg/L, 540 mg/L and 1180 mg/L in WA20, WA50 and WA80 reactors.

3.2. Batch tests: comparative efficiency of dispersed alkaline substrates

Over the batch testing duration, three periods have generally been observed in the evolution of treated water quality in reactors: 1) optimal efficiency (0–21 days), 2) steady state (21–70 days), and 3) either steady state or efficiency improvement (70–91 days).

3.2.1. First period (0–21 days) – optimal efficiency

During this period, water pH increased in all reactors (from 4 to an average of 6.7, 5.4, 4.8 in WA-, calcite- and dolomite-DAS reactors, respectively), regardless of the proportion of neutralizing

agents in the DAS mixtures. However, in the WA-DAS reactors, pH was higher than either calcite- or dolomite-DAS, due to the higher neutralizing capacity of wood ash, especially within the first week (Fig. 1). The Eh decreased from 405 mV to slightly lower values (around 290 mV) in calcite- and WA-DAS comparing to that of dolomite-DAS (326 mV), showing oxic condition (Fig. 1).

In the same time, the WA-DAS neutralized during the first 14 days up to 96% of acidity, whereas calcite- and dolomite-DAS neutralized only 16–27% (Fig. 1). After day 21, the acidity increased in WA-DAS, C20 and C80, which is partially explained by the additional acidity generated during the fast precipitation of Fe (oxy)-hydroxide. Similar results have been previously reported, when alkaline materials with small grain size were used in a limestone-DAS (Ayora et al., 2013). From the first 7 days, the alkalinity increased significantly in the WA-DAS (on average 1240 mg/L as $CaCO_3$) and calcite-DAS (230 mg/L as $CaCO_3$), but not with the dolomite-DAS (0–5 mg/L as $CaCO_3$) (Fig. 1).

The low value of alkalinity obtained in the last reactors is consistent with the low recorded pH values and was expected, considering the low reactivity of dolomite. However, at the end of this first period, while alkalinity decreased rapidly in the WA- and calcite-DAS (286 mg/L as $CaCO_3$ and between 17 and 37 mg/L as $CaCO_3$, respectively), it increased in the dolomite-DAS reactors (between 4.5 and 11.5 mg/L as $CaCO_3$), which means that dolomite started to be activated only after 21 days.

As the pH increased rapidly because of the fast reactivity of the wood ash, precipitates assumed to be ferric hydroxide (likewise visible as yellow, yellow-brown in the WA-DAS reactors during this experiment) appeared. In addition, because of the high Fe concentration, the precipitation of ferric hydroxide occurred firstly, thereby influencing gypsum precipitation, especially when the ratio Ca^{2+}/SO_4^{2-} was low. In such cases, Fe oxide-hydroxides (instead of gypsum) armoring could be the major issue during the passive treatment of Fe-rich AMD. However, Fe oxide-hydroxides are weakly bound precipitates and can be removed mechanically or flushed (Santomartino and Webb, 2007; Wolfe et al., 2010). Given their positive charged surfaces at pH < 8, they could potentially sorb oxy-anions of As and Sb, if present in the AMD (Cornell and Schwertmann, 2003; Sparks, 2003).

The DO remained high in all reactors during the first 7 days (~8.1 mg/L), which may partially explain the optimal Fe removal of the treatment, particularly in WA-DAS reactors during this period, since it contributed to oxidation, hydrolysis and precipitation of Fe^{2+} (Strosnider et al., 2013). As a result, Fe removal with the WA-DAS was up to 99.9% (Fig. 1), corresponding to 1680 mg Fe, at a rate of 238 mg Fe/d (Table 2, Supplementary material). Resultant SO_4^{2-} removal was between 25 and 44%, with WA20 and WA80 as the most and the least efficient, respectively (Fig. 2). However, after 21 days, the DO dropped to 0.80–1.29 mg/L in all reactors, probably due to organic matter decomposition (Sahoo et al., 2013). This was followed by a slight decrease in Fe removal to 94% (Fig. 1), while SO_4^{2-} removal remained constant (Fig. 2). Hence, Fe and/or SO_4^{2-}

Table 4
DAS systems efficiency during the steady state of ferriferous AMD treatment.

Parameters	WA-DAS	Calcite-DAS	Dolomite-DAS
pH	6.65	5.62	5.08
Eh (mV)	232	220	274
DO (mg/L)	0.95–1.15	1.05–1.28	1.67–2.22
Alkalinity (mgCaCO₃/L)	423–710	33–95	23–53
Acidity (mgCaCO₃/L)	320–510	2600	2630
Fe removal (%)- AMD <1500 mg/L	91	29	27
Fe removal (%)- AMD >1500 mg/L	90	17	D20: 8%; DAS >50% dolomite: 23%
SO_4^{2-} removal (%)	18–40	<10 except C80 (31%)	<10

reduction is not excluded. Nonetheless, with sufficient alkalinity to buffer the acid and maintain high pH values (>3.5), the main removal mechanism of Fe is the precipitation in the form of oxide-hydroxides and carbonates. Sorption and co-precipitation mechanisms can also occur.

The efficiency of calcite- and dolomite-DAS was related to their reactivity. The fast reactivity of calcite during the first stage of dissolution, which is correlated to the neutralization of sulfuric acid (Maree et al., 1992; Potgieter-Vermaak et al., 2006), ascribed calcite-DAS its capacity to early increase the pH, and thus precipitate metals. Accordingly, calcite-DAS allowed maximal Fe_t removal up to 66% after 14 days, whereas in this same period, dolomite-DAS removed only 22%, on average (Fig. 1).

Additionally, SO_4^{2-} removal was comparable for the two types of DAS (29% for C20 and D20; 40% for DAS with $\geq$50% of calcite or dolomite). Within the first 7 days of the batch testing with calcite- and dolomite-DAS, SO_4^{2-} concentration increased, except in C20. The release of SO_4^{2-} originating in the materials constituting the mixtures could contribute to this increase (Neculita and Zagury, 2008). Indeed, control batch reactor containing W20, which SO_4^{2-} content was the same as calcite- and dolomite-DAS mixtures, showed release of 220 mg/L SO_4^{2-} (Table 3). This could explain also the decrease of SO_4^{2-} removal in all calcite- and dolomite-DAS reactors to <12% after 21 days. Hence, a proportion of 50% of calcite or dolomite could be enough for ferriferous AMD (with Fe < 1500 mg/L) pre-treatment only within short period of times because after the first 7 days, C80 and D80 showed the lowest Fe^{2+} removal (<5% efficiency) (Fig. 1). Gypsum precipitation probably hindered acid neutralization and, thus, Fe concentration stayed high. Geochemical modeling using water chemistry on day 7, from reactors C80 and D80, supports this hypothesis by indicating gypsum oversaturation and the possible subsequent precipitation.

Saturation indices (SI) calculated with VMINTEQ using water chemistry in all reactors on days 0,7, 14 and 21 indicated oversaturation of oxide-hydroxide minerals, such as $Fe_3(OH)_{8\ (s)}$, goethite (α-FeOOH), hematite (α-Fe$_2$O$_3$), H-jarosite [(H$_3$O)

$Fe_3(OH)_6(SO_4)_2$], lepidocrocite (γ- FeOOH) and magnetite (Fe$_3$O$_4$). Fe would be also precipitated under the form of Fe-carbonate siderite (FeCO$_3$) in the WA-DAS reactors.

3.2.2. Second period (21—70 days) — steady state

The pH in calcite- and WA-DAS reactors remained stable, while it increased to 5.12 in dolomite-DAS, but not in D80 (pH 4.99). The overall increase of pH value in all reactors seemed independent of the neutralizing agent proportion in the tested DAS; however, this could play a key role in the long term sustainability of their performance. Other parameters indicating water quality such as Eh, EC, and DO followed similar trends, and showed slight decrease or stability in all reactors (Table 4).

The alkalinity stayed high in WA-DAS reactors (81—1407 mg/L as CaCO$_3$), accompanied with a decrease in acidity down to 37.5% (final values 134—717 mg/L as CaCO$_3$). Subsequently, Fe_t removal was maintained relatively high to approximately 90%, giving a cumulative precipitation of 1700 mg Fe, at a rate of 240 mg Fe/d (Table 2, Supplementary material). The mechanism of Fe removal in WA-DAS was mainly the oxide-hydroxides precipitation. Ion exchange, as well as adsorption could also occur according to previous studies on the Fe removal with wood ash (Genty et al., 2012b). At the end of the experiment, the Ss of WA20, WA50 and WA80 decreased respectively to 5.68 m^2/g, 16.76 m^2/g, and 30.08 m^2/g.

The efficiency of calcite- and dolomite-DAS was comparable, with an average removal of 28% Fe. According to Fe^{2+} removal, treatment of ferriferous AMD contaminated with Fe < 1500 mg/L, was around 17% in calcite-DAS reactors, 8% in D20 and ~23% in D50 and D80 (Table 4).

The similar performance of the calcite- and dolomite-DAS could be explained by the slower Fe removal in the calcite-DAS due to coating of calcite grains by precipitates, which corresponds to the second stage of calcite neutralization (Maree et al., 1992; Potgieter-Vermaak et al., 2006). The SO_4^{2-} removal was 18—40% with WA-DAS, whereas it was below 10% with calcite- and dolomite-DAS, except in C80 (31%). Irregularities in SO_4^{2-} removal are not easy to
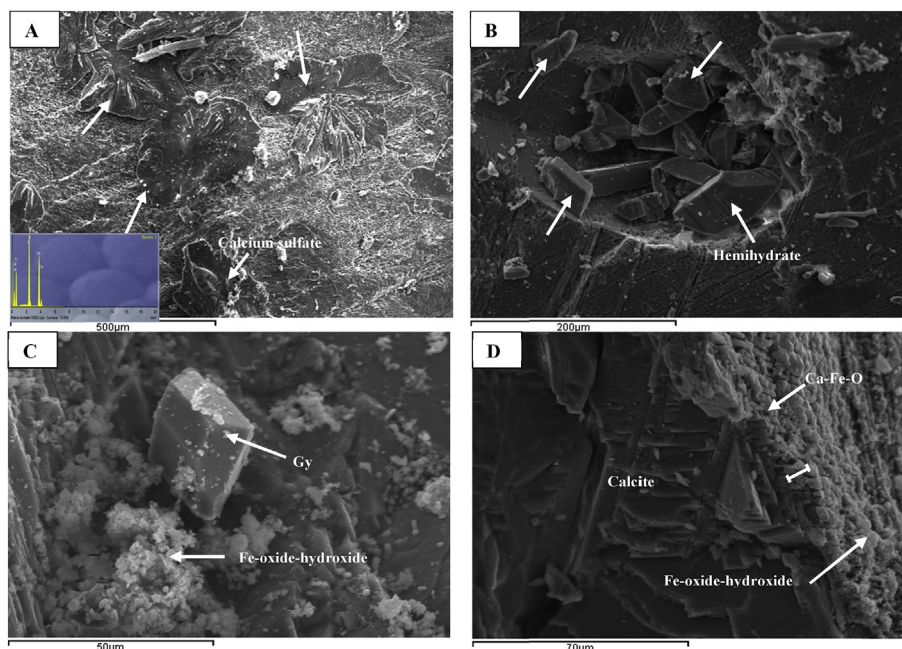

Fig. 3. SEM-EDS images of the surface of calcite from C20 (cal-C20) and C80 (cal-C80) after the treatment: (A) Surface of cal-C20 covered by patch-like calcium sulfate on a layer of Fe/Al- oxyhydroxide, (B) Niche filled with gypsum crystals on the surface of cal-C20, (C) Monoclinic gypsum and flaky Fe-oxyhydroxide on the surface of the cal-C80, (D) Cal-C80 fouled with ~5 μm of Fe-oxide-hydroxides and srebrodolskite.

explain, but were consistent with similar DAS-based treatment systems using calcite or dolomite (e.g. Rötting et al., 2008a; Ayora et al., 2013). Nonetheless, SO_4^{2-} could be also removed as calcium sulfate, such as anhydrite and gypsum, as well as sorption onto Fe-oxide-hydroxides. Indeed, SI calculated with VMINTEQ using water chemistry on days 21, 35, 56, 70 indicated the oversaturation of (oxy) hydroxide minerals, as well as of gypsum. The Fe-oxide-hydroxides, which were identified as the yellow-brown precipitates on the bottom of the reactors, could be responsible for calcite and dolomite armoring, and the decrease of their dissolution and reactivity.

3.2.3. Third period (70–91 days) – steady state or efficiency improvement

The WA-DAS maintained their performance and the steady state period was extended to the third phase, whereas the efficiency of calcite- and dolomite-DAS was enhanced. Consequently, the pH, Eh, and EC showed stability or water quality improvement. The pH remained constant in all reactors except for D80, in which it slightly increased from 4.99 to 5.33 units. The EC dropped from 2.52 mS/cm to 1.95 mS/cm and <1 mS/cm in WA-DAS and both calcite- and dolomite-DAS, respectively, presenting a decrease of the total dissolved solid. The proportion of neutralizing agents seemed to be linked with the generated alkalinity, which augmented around 13% in the reactors containing <50% of wood ash, and 40% in WA80. Consequently, the neutralized acidity was on the one hand 4% in WA20, 21% in WA50 and 36% in WA80. On the other hand, acidity in dolomite-DAS reactor was slightly lower (950–2750 mg/Las $CaCO_3$) than in calcite-DAS reactors (1287–2872 mg/L as $CaCO_3$). It is worth mentioning that alkalinity in dolomite-DAS constantly increased until the end of the experiments (up to 86%), which could be advantageous to reduce acidy in long term (Fig. 1). The low value of DO (0.18–1.2 mg/L) in all reactors suggested that oxidation of Fe^{2+} was spurred by other processes for example sufficient alkalinity that buffers the acidic solution (Younger et al., 2002). Indeed, correlated with acidity neutralization rate, Fe removal slightly decreased in WA20 (85%, final value 350 mg/L), while it stayed constant in WA50 (90%, final value 235 mg/L) and increased in WA80 (97%, final value 75 mg/L) (Fig. 1). Generally, Fe removal of calcite- and dolomite-DAS was improved and increased to about 33% in reactors with ≤50% calcite or dolomite, 49% in C80 and 66% in D80. Based on the results of Fe^{2+} removal, all tested DAS could pre-treat Fe-rich AMD with Fe < 1500 mg/L, with an efficiency of 93% (around 94 mg/L) in WA-DAS, ~50% (670 mg/L) in calcite-DAS and between 43 and 67% (440–770 mg/L) in dolomite-DAS (Fig. 1). The DAS systems with ≥50% of dolomite seems particularly promising because in D50 and D80, Fe concentration

decreased to 386 mg/L and 290 mg/L, respectively, after day 84. However, a larger system and a longer hydraulic retention time would be necessary.

The efficiency improvement of the calcite- and dolomite-DAS reactors over time could be due to the reactivation of calcite and/or dolomite grains after passivation with Fe precipitates. The interaction of acidic solution with the calcite or dolomite grains in the DAS mixtures led to dissolution of secondary Fe minerals from the armored grains surface. Thereby, the effective surface area would be reactivated. Indeed, the surface area of the calcite- and dolomite-DAS mixture after the treatment increased up to 5 times their initial values. Hence, sorption could occur as metal removal mechanism. Moreover, the coating/dissolution phenomenon would influence the effectiveness of the DAS mixtures. Some other studies corroborated this fact and stated that efficiency of armored and unarmored limestone was comparable as dissolution of grains increases with acidity in the solution (Ziemkiewicz et al., 1997; Simón et al., 2005). In addition, as pH remained constant (4–5), the acidity neutralization stayed constant (Ziemkiewicz et al., 1997).

Improvement of SO_4^{2-} removal required longer contact time according to the efficiency of the different mixtures (31–49% in WA-DAS, 14–35% in calcite-DAS, <10% in dolomite-DAS reactors) (Fig. 2). The calcite- or dolomite-DAS required also longer contact time relative to wood ash.

3.3. Removal of other metals

All mixtures removed up to 92% Al. According to the modeling results (i.e. VMINTEQ) on water quality from days 0 and 91, Al-oxide-hydroxides such as diaspore [AlO(OH)], [Al(OH)$_3$], and hydrated aluminium sulfate basaluminite [Al$_4$(OH)$_{10}$SO$_4$] were oversaturated. The DAS composed of wood ash and those with more than 50% of calcite allowed >90% of Zn removal, while the dolomite-DAS removed only 23% and 76% of Zn in D50 and D80, respectively. The Pb removal was 88% in W20, >94% in WA50 and W80, 41–68% in calcite-DAS and 33–78% in dolomite-DAS. These results showed that at a very low concentration, Zn and Pb removal appears to be strongly linked to alkaline agent proportion in the mixtures, and pH values. The higher is the amount of alkaline agent, the longer the pH is maintained at a value that promotes higher removal rate, with respect to concentration. Moreover, since results of modeling indicated that Pb was mostly removed as PbCO$_3$, the lower Pb removal in the calcite- and dolomite-DAS could have been explained by coating of grains that limited dissolution and availability of HCO$_3^-$/CO$_3^{2-}$. The Mn was not removed except in WA50 (up to 50%). Factors such as pH, DO, surface of Mn- and Fe-oxides and the presence of reducing agents, such as Fe^{2+} could adversely
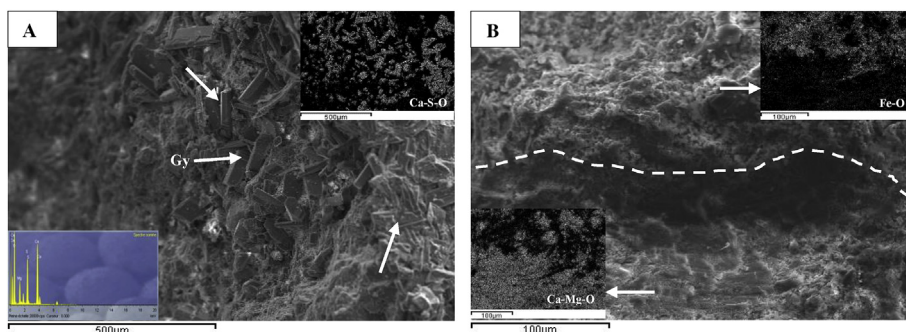

Fig. 4. SEM-EDS images of the surface of dolomite from D20 (dol-D20) and D80 (dol-D80) after the treatment: (A) Surface of dol-D20 covered by gypsum (Gy) and Fe-oxide-hydroxides, (B) Layer of ~50 μm of precipitates (srebrodolskite, portlandite) and Fe-oxide-hydroxides on the surface of the dol-D80.

impact Mn removal (Rose et al., 2003; El Gheriany et al., 2009). The evaluation of key parameters influencing Mn removal in the presence of high concentrations of Fe requires further study.

3.4. Post-testing mineralogy

The precipitates on the surface of the mixtures composed of 20% and 80% of neutralizing agents (WA20, WA80, C20, C80, D20, and D80), after the batch testing, have been observed with SEM-EDS. The main mineral phases consisted of calcium sulfate, mainly gypsum, and Fe-oxide-hydroxides. The surface of the calcite recovered from the spent mixture C20 (cal-C20) was covered by a patch-like calcium sulfate (Fig. 3A). The formation of this latter may be due to its direct contact to sulfuric acid and organic colloids from the decomposition of organic matter, which were both found to be as calcium sulfate crystal growth inhibitors (Singh and Middendorf, 2007). This hypothesis could be corroborated by the fact that gypsum crystals could grow in the niche of the calcite grains (Fig. 3B). It appears then that the high acidity and the pore volume of the calcite grains might influence the growth of crystal gypsum. Indeed, at a lower acidity, gypsum crystal could develop as it has been observed on the surface of the calcite from C80 (cal-80) (Fig. 3C). Similarly to what was found on cal-C20, crystals of gypsum were well formed in the hollow of dolomite grains from D20

(dol-D20) (Fig. 4A). Whilst gypsum reached saturation (as it has been modelled), calcite and/or dolomite continued to be dissolved, adding Ca and Mg that would become oversaturated and precipitated as portlandite [$Ca(OH)_2$]. The Fe was detected in the form of siderite, chukanovite [$Fe_2(CO_3)(OH)_2$], srebrodolskite ($Ca_2Fe_2O_5$), magnesioferrite ($MgFe_2O_4$), and hydroniumjarosite [$(H_3O)Fe_3(SO_4)_2(OH)_6$]. The layer thickness of the secondary precipitates on the surface of calcite and dolomite grains was between 5 and 50 μm, which could impede further reactivity (Figs. 3D, 4B, Fig. 1, Supplementary material).

The surface of wood chips recovered from WA20 was partially enveloped by secondary precipitates of Fe-oxide-hydroxides (Fig. 5A). On the contrary, that of WA80 was completely coated (Fig. 5B). This is in accordance to the amount of precipitated Fe which was higher in WA80 than in W20 reactor. Poorly crystallized, plate and small particles of hemihydrate gypsum was observed on wood chips from C20 (Fig. 5C). On the surface of wood chips from C80, amorphous Fe-oxide-hydroxides were more abundant than gypsum (Fig. 5D). The hydration of calcium sulfate hemihydrate formed needle shape gypsum on the surface of wood chips from D20. The particle size of gypsum precipitated in the D80 varied from 5 to 150 μm. The large interlocked gypsum indicates the hydration of hemihydrate which could have been influenced by pH, acid concentration, and temperature (Fig. 5F).
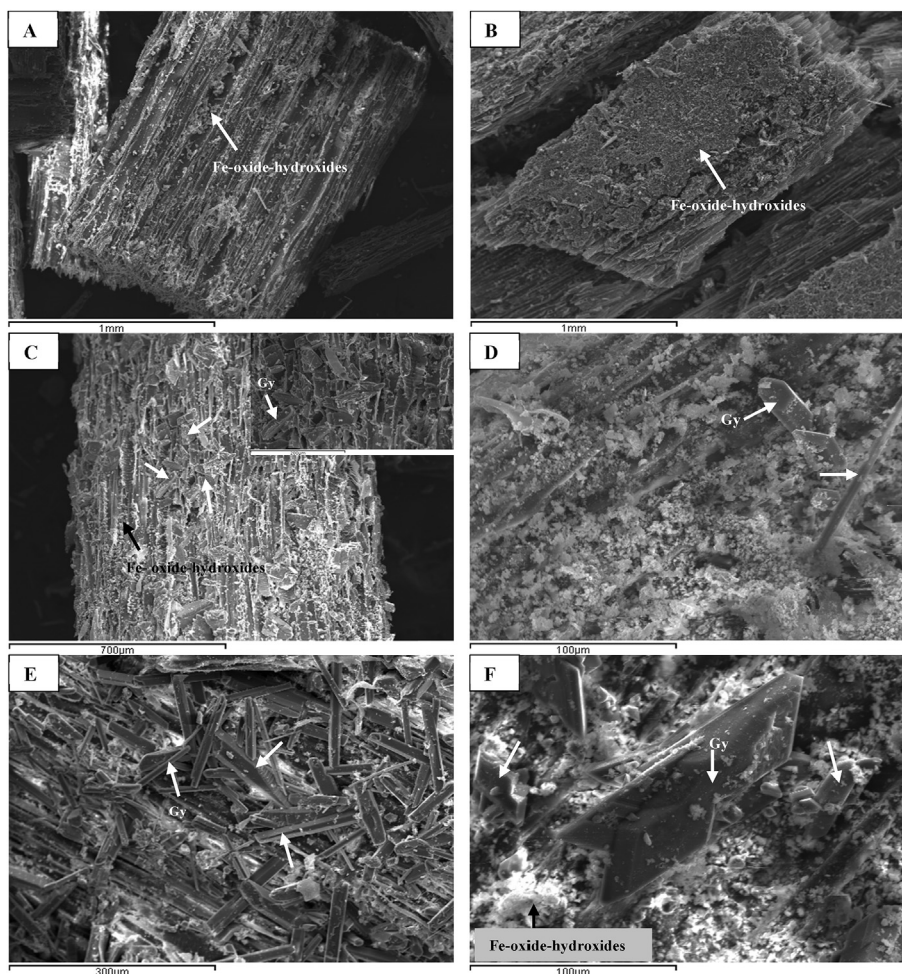

Fig. 5. SEM-EDS images of wood chips recovered from mixtures after the batch testing and fouled with precipitates: (A) Wood chips from WA20 partially covered by Fe-oxyhydroxide, (B) Wood chips from WA80 with all the surface patched with Fe-oxyhydroxide, (C) Wood chips from C20 fouled with plate small grains of needle shaped hemihydrate gypsum (Gy) with local precipitates of Fe-oxide-hydroxides, (D) Wood chips from C80 fouled with Fe-oxide-hydroxides with euhedral and needle shaped gypsum, (E) Wood chips from D20 covered with needle shaped-gypsum, (F) Wood chips from D80 covered with a layer of Fe-oxide-hydroxides under variable size (5 μm—150 μm) of euhedral gypsum.
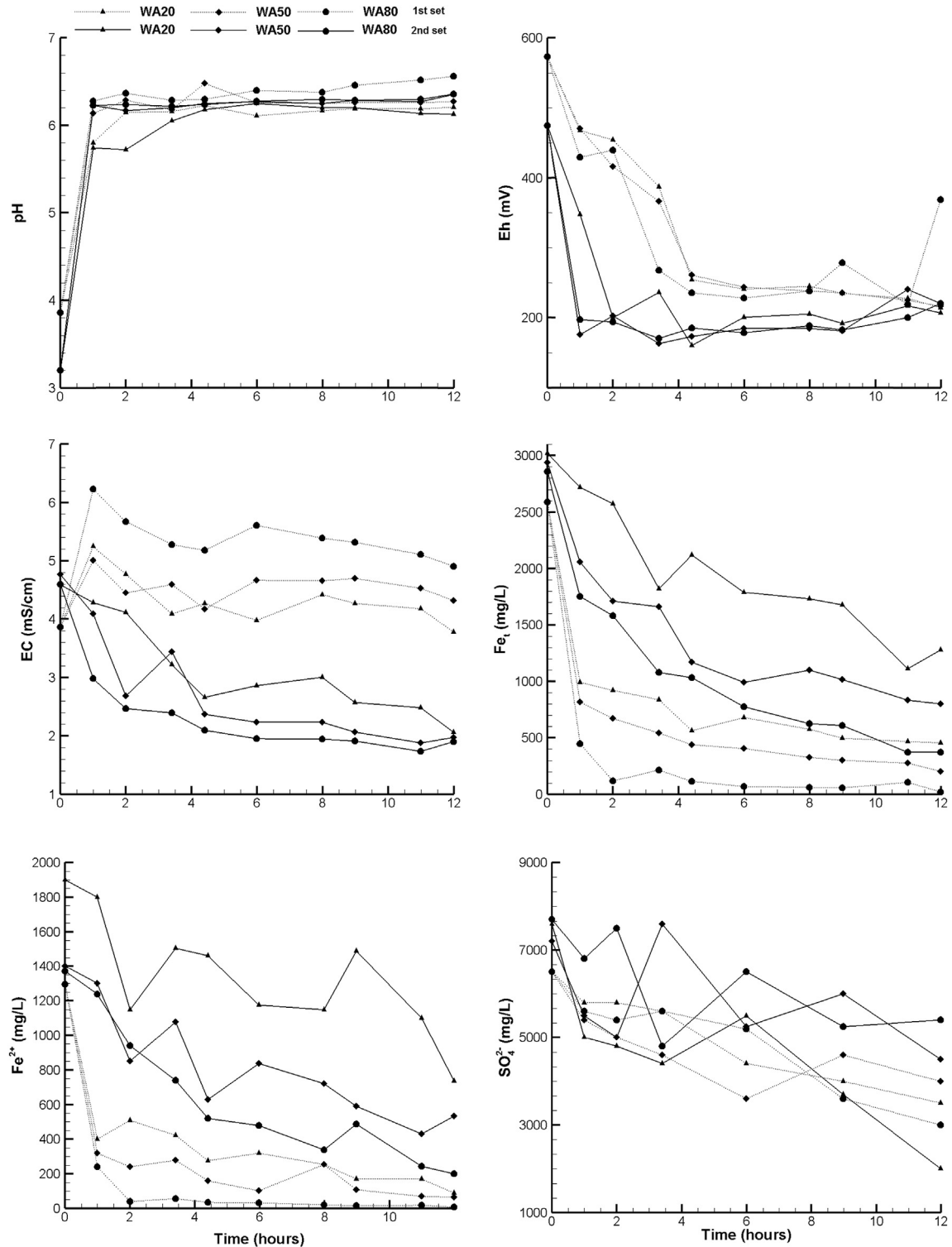
Fig. 6. Evolution of Fe_t, Fe^{2+} and SO_4^{2-} concentrations in the first 12 h of treatment in WA-DAS.

It can be concluded that the precipitation and sorption of secondary minerals on the wood chips surface can limit coating of calcite or dolomite grains. With 20% of neutralizing agent, gypsum precipitation is favored while with 80%, Fe-oxide-hydroxides are more abundant.

In order to optimize the XRD analysis (detection limit <1% w/w), two spent reactive mixtures (WA50 and D50) were selected. The presence of goethite, lepidocrocite as well as gypsum were principally the expected mineral phases. The XRD analysis showed that gypsum was the main crystallized secondary mineral. Quartz and

biotite originating from the mixtures were also identified. The presence of pyrite was also detected, indicating that Fe^{3+} and SO_4^{2-} reduction occurred (Fig. 2, Supplementary material). However, Fe-oxide-hydroxides were amourphous and could not be detected.

3.5. Performance of wood ash type DAS: iron removal within the first 12 h

As noted during the 91 days of batch testing, efficient Fe removal in mixtures containing wood ash occurred within the first 7 days. To better evaluate the critical time where Fe decreased to under 500 mg/L, and to better assess the efficiency of each of the three WA-DAS, three batch reactors containing WA20, WA50 and WA80 were set up as the previous tests (1 L glass flasks filled with 200 g dry mixture and 600 mL of synthetic AMD). Two sets of tests were undertaken where Fe_t, Fe^{2+} and SO_4^{2-} removal was mainly measured within the first 12 h, using the same analysis methods as the 91-day period batch test. After the first 12 h test, a second set was carried out with the AMD concentration set back at the initial concentration (2500 mg/L Fe).

During the first set of tests, the pH increased after 1 h from 3.86 to 5.8, 6.14, and 6.28 in WA20, WA50, and WA80, respectively, and maintained stable around 6.30 in all reactors after 12 h (Fig. 6). The Eh was around 300 mV, indicating an oxic environment (Fig. 6). The EC in WA20 and WA50 was 4.45 mS/cm, whereas that of WA80 was 5.4 mS/cm, which was explained by the high content in dissolved suspended solids (Fig. 6).

The efficiency of the three WA-DAS showed distinctive features, with Fe concentration in the reactors decreasing from 2590 mg/L to 495 mg/L after 9 h, to 440 mg/L after 4 h, and to 450 mg/L after 1 h, in WA20, WA50 and WA80, respectively (Fig. 6), corresponding to around 1300 mg Fe removal in each of the reactor (Table 3, Supplementary material). The Fe^{2+} concentrations were 170 mg/L in WA20, 160 mg/L in WA50 and 240 mg/L in WA80 (Fig. 6), with similar precipitation rate (Table 3, Supplementary material). After 12 h, SO_4^{2-} concentration decreased from 6500 mg/L to around 4700 mg/L.

On the second set of experiments, the pH was similar to the first set and the Eh decreased to 200 mV. The EC also decreased to around 2.4 mS/cm in all reactors (Fig. 6).

Fe removal trend was the same as the first run for all reactors, except that Fe decreased at less than 500 mg/L only after 12 h in WA20, 11 h in WA50 and 6 h in WA80 (Table 4, Supplementary material). Thus, longer contact time was required for the first two DAS to decrease Fe concentration. Overall, Fe^{2+} concentration decreased to <500 mg/L after 12 h in WA20 (420 mg/L), and after 4 h in WA50 and W80 (340 mg/L and 260 mg/L) (Fig. 5). Thus, for the pre-treatment of ferriferous AMD, a contact time of 4 h would be enough if Fe < 1500 mg/L, and 6–11 h if Fe > 1500 mg/L.

The SO_4^{2-} removal in WA20 (44%) was better than in WA50 (25%) and in WA80 (19%). Thus, WA20 appears to be promising. Nonetheless, alkalinity generation could be limited, therefore limiting long term performance of the treatment system. However, the use of WA80 involves higher content of fine grains, leading to a possible long term decline in hydraulic conductivity and limitation of efficiency. Given the obtained results and the advantage of WA-DAS to rise water pH around neutral (maximal 7.12), which does not require adjustment when used in a polishing or pre-treatment unit, oppositely to MgO-DAS, the WA50 seems to be the best compromise between the three WA-DAS.

4. Conclusion

The present study evaluated three types of DAS (dispersed alkalinity substrate), comprised of natural alkaline materials (wood ash, calcite, dolomite) in different proportions (20% v/v, 50% v/v, 80% v/v), and substrate with high surface area (wood chips) in 9 batch reactors, for Fe pre-treatment in ferriferous AMD (>1500 mg/L Fe), over a 91-day period. Among the tested DAS, the one composed of wood ashes (WA) was the most effective (99.9%), whereas those containing calcite or dolomite gave comparable performance. A contact time of 6–11 h was required for Fe concentrations to be decreased to below 500 mg/L. The efficiency of the WA-DAS systems was similar, regardless of the proportion of wood ash. However, the possible washing out/clogging because of the high content of fine particles of W80, as well as the rapid alkalinity depletion of WA20, that eventually lead to limited long term performance, pointed out WA50 as the best choice for Fe pre-treatment. In a very short term run, calcite-DAS was more efficient (66%) than dolomite-DAS (22%). However, in a mid-term, calcite- and dolomite-DAS could be potentially substituted and used in a polishing unit for the passive treatment of iron-rich AMD. All DAS mixtures showed Al, Zn and Pb removal, except for Mn, which was removed up to 50% only in WA50. SO_4^{2-} removal in WA-DAS was higher (18–40%) compared to calcite- or dolomite-DAS (<10%). Nonetheless, additional treatment units for sulfate removal are necessary.

Acknowledgements

Appendix A. Supplementary data

Supplementary data related to this article can be found at http://dx.doi.org/10.1016/j.apgeochem.2016.07.014.

References

Aitcin, P.C., Généreux, F., Jolicoeur, G., Maurice, M., 2012. Technologie des granulats, third ed., p. 352 Modulo, Montréal, QC (Canada).

APHA (American Public Health Association), 2005. Titration method. In: Greenberg, A. (Ed.), Standard Methods for the Examination of Water and Wastewater, nineteenth ed., pp. 161–166 Washington, DC (USA).

ASTM (American Society for Testing and Materials), 1995. Standard Test Method for Permeability of Granular Soils. Annual book of ASTM Standards.08. D 2434 – 68, Philadelphia, PA (USA).

Asadi, A., Huat, B.K.B., Hanafi, M.M., Mohamed, T.A., Shariatmadari, N., 2009. Role of organic matter on electroosmotic properties and ionic modification of organic soils. Geosci. J. 13 (2), 175–181.

Ayora, C., Caraballo, M.A., Macías, F., Rötting, T.S., Carrera, J., Nieto, J.-M., 2013. Acid mine drainage in the Iberian Pyrite Belt: 2. Lessons learned from recent passive remediation experiences. Environ. Sci. Pollut. Res. 20, 7837–7853.

Bejan, D., Bunce, N.J., 2015. Acid mine drainage: electrochemical approaches to prevention and remediation of acidity and toxic metals. J. Appl. Electrochem. 45, 1239–1254.

Caraballo, M.A., Macías, F., Rötting, T.S., Nieto, J.M., Ayora, C., 2011. Long term remediation of highly polluted acid mine drainage: a sustainable approach to restore the environmental quality of the Odiel river basin. Environ. Pollut. 159, 3613–3619.

Champagne, P., Van Geel, P., Parker, W., 2008. Impact of temperature and loading on the mitigation of AMD in peat biofilter columns. Mine Wat. Environ. 27, 225–240.

Cornell, R.M., Schwertmann, U., 2003. The Iron Oxides: Structure, Properties, Reactions, Occurrences, and Uses, second ed. Wiley-VCH GmbH&Co. KGaA, Weinheim (Germany), p. 694.

El Gheriany, I.A., Bocioaga, D., Hay, A.G., Ghiorse, W.C., Shuler, M.L., Lion, L.W., 2009. Iron requirement for Mn(II) oxidation by *Leptothrix discophora* SS-1. Appl. Environ. Microbiol. 1229–1235.

Figueroa, L., Miller, A., Zaluski, M., Bless, D., 2007. Evaluation of a two-stage passive treatment approach for mining influenced waters. In: National Meeting of the American Society of Mining and Reclamation (ASMR), Gillette, WY, 30 Years of SMCRA and beyond. June 2-7, Barnishel, R.I., Lexington, KY (USA), pp. 238—247.

Genty, T., Bussière, B., Zagury, G.J., Benzaazoua, M., 2010. Passive treatment of high-iron acid mine drainage using sulphate reducing bacteria: comparison between eight biofilter mixtures. In: Wolkersdorfer & Freund (Ed.), Proceed. of the International Mine Water Association (IMWA), pp. 229—232. September 5-9, Sydney, NS (Canada).

Genty, T., Bussière, B., Potvin, R., Benzaazoua, M., Zagury, G.J., 2012a. Dissolution of calcitic marble and dolomitic rock in high iron concentrated acid mine drainage: application to anoxic limestone drains. Environ. Earth. Sci. 66, 2387—2401.

Genty, T., Bussière, B., Potvin, R., Benzaazoua, M., Zagury, G.J., 2012b. Capacity of wood ash filters to remove iron from acid mine drainage: assessment of retention mechanism. Mine Water. Environ. 31 (4), 273—286.

Hedin, R., Weaver, T., Wolfe, N., Watzlaf, G., 2013. Effective passive treatment of coal mine drainage. In: Proceed. of the 35th Annual National Association of Abandoned Mine Land Programs Conference, September 22—25, Daniels, WV (USA), p. 13.

Huminicki, D.M.C., Rimstidt, J.D., 2008. Neutralization of sulfuric acid solutions by calcite dissolution and the application to anoxic limestone drain design. Appl. Geochem. 23, 148—165.

Jennings, S.R., Jacobs, J.A., 2014. Overview of acid drainage prediction and prevention. In: Jacobs, J.A., Lehr, J.H., Testa, S.M. (Eds.), Acid Mine Drainage, Rock Drainage, and Acid Sulfate Soils: Causes, Assessment, Prediction, Prevention, and Remediation. John Wiley & Sons, Inc., Hoboken, NJ (USA), pp. 205—215.

KTH, 2013. Visual MINTEQ, Version 3.0: a Window Version of MINTEQA2 available at: http://vminteq.lwr.kth.se/ (last access: 8 August 2015).

Lozano, A., Ayora, C., Macias, F., Nieto, J.M., Gomez-Arias, A., Castillo, J., Van Heerden, E., 2015. Sulphate removal from acid mine drainage: evaluation of granular BaCO$_3$ with column experiments. Macla 20, 83—84.

Macías, F., Caraballo, M.A., Rötting, T.S., Péréz-López, R., Nieto, J.M., Ayora, C., 2012. From highly polluted Zn-rich acid mine drainage to nonmetallic waters: implementation of multi-step alkaline treatment system to remediate metal pollution. Sci. Total Environ. 435, 323—350.

Maree, J.P., Du Plessis, P., Van der Walt, C.J., 1992. Treatment of acidic effluents with limestone instead of lime. Water Sci. Technol. 26 (1—2), 345—355.

Neculita, C.M., Zagury, G.J., 2008. Biological treatment of highly contaminated acid mine drainage in batch reactors: long-term treatment and reactive mixture characterization. J. Hazard. Mater. 157, 358—366.

Neculita, C.M., Zagury, G.J., Bussiere, B., 2008. Effectiveness of sulphate-reducing passive bioreactors for treating highly contaminated acid mine drainage: I. Effect of hydraulic retention time. Appl. Geochem. 23, 3442—3451.

Neuman, D.R., Brown, P.J., Jennings, S.R., 2014. Metals associated with acid rock drainage and their effect on fish health and ecosystems. In: Jacobs, J.A., Lehr, J.H., Testa, S.M. (Eds.), Acid Mine Drainage, Rock Drainage, and Acid Sulfate Soils: Causes, Assessment, Prediction, Prevention, and Remediation. John Wiley & Sons, Inc., Hoboken, NJ (USA), pp. 139—169.

Nordstrom, K., Blowes, D.W., Ptacek, C.J., 2015. Hydrogeochemistry and microbiology of mine drainage: an update. Appl. Geochem. 57, 3—16.

Potgieter-Vermaak, S.S., Potgieter, J.H., Monama, P., Van Grieken, R., 2006. Comparison of limestone, dolomite and fly ash as pre-treatment agents for acid mine drainage. Min. Eng. 19, 454—462.

Potts, P.J., 1987. A Handbook of Silicate Rock Analysis. Blakie & Son Ltd, p. 622.

Rötting, T.S., Jordi, C., Ayora, C., 2006. Use of caustic magnesia to remove cadmium, nickel, and cobalt from water in passive treatment systems: column experiments. Environ. Sci. Technol. 40, 6438—6443.

Rötting, T.S., Thomas, R.C., Ayora, C., Carrera, J., 2008a. Passive treatment of acid mine drainage with high metal concentrations using dispersed alkaline substrate. J. Environ. Qual. 37, 1741—1751.

Rötting, T.S., Caraballo, M.A., Serrano, J.A., Ayora, C., Carrera, J., 2008b. Field application of calcite Dispersed Alkaline Substrate (calcite-DAS) for passive treatment of acid mine drainage with high Al and metal concentrations. Appl. Geochem. 23, 1660—1674.

Rose, A.W., Means, B., Shah, P.J., 2003. Methods for passive removal of manganese from acid mine drainage. In: Proceed. of West Virginia Surface Mine Drainage Task Force Symposium, Morgantown, WV (USA), p. 11.

Sahoo, P.K., Kim, K., Equeenuddin, Sk.Md., Powell, M.A., 2013. Current approaches for mitigating acid mine drainage. In: Whitacre, D.M., Bennett, E.R., Doerge, D.R. (Eds.), Reviews of Environmental Contamination and Toxicology, vol. 226, pp. 1—22. NY (USA).

Santomartino, S., Webb, J.A., 2007. Estimating the longevity of limestone drains in treating acid mine drainage containing high concentrations of iron. Appl. Geochem. 2, 2344—2361.

Simón, M., Martín, F., García, I., Bouza, P., Dorronsoro, C., Aguilar, J., 2005. Interaction of limestone grains and acidic solutions from the oxidation of pyrite tailings. Environ. Pollut. 135 (1), 65—72.

Singh, N.B., Middendorf, B., 2007. Calcium sulphate hemihydrate hydration leading to gypsum crystallization. Prog. Cryst. Growth Charact. Mater. 53, 57—77.

Sparks, D.L., 2003. Environmental Soil Chemistry, second ed. Academic Press, San Diego, CA (USA), p. 352.

Strosnider, W.H.J., Nairn, R.W., Peer, R.A.M., Winfrey, B.K., 2013. Passive co-treatment of Zn-rich acid mine drainage and raw municipal wastewater. J. Geochem. Explor. 125, 110—116.

USEPA (United States Environmental Protection Agency), 2014. Reference Guide to Treatment Technologies for Mining-influenced Water. EPA 542-R-14—001, p. 94.

Wolfe, N., Hedin, B., Weaver, T., 2010. Sustained treatment of AMD containing Al and Fe^{3+} with limestone aggregate. In: Wolkersdorfer & Freund (Ed.), Proceed. of the IMWA, September 5-9, pp. 29—32. Sydney, NS (Canada).

Younger, P.L., Banwart, S.A., Hedin, R.S., 2002. Passive treatment of polluted mine waters. In: Mine Water: Hydrology, Pollution, Remediation. Kluwer Academic Publishers, Norwell, MA (USA), pp. 311—393.

Ziemkiewicz, P.F., Skousen, J.G., Brant, D.T., Sterner, P.L., Lovett, R.J., 1997. Acid mine drainage treatment with armored limestone in open channels. J. Environ. Qual. 26 (4), 1017—1024.

Zipper, C., Skousen, J., 2014. Passive treatment of acid mine drainage. In: Jacobs, J.A., Lehr, J.H., Testa, S.M. (Eds.), Acid Mine Drainage, Rock Drainage, and Acid Sulfate Soils: Causes, Assessment, Prediction, Prevention, and Remediation. John Wiley & Sons, Inc., Hoboken, NJ (USA), pp. 339—353.